http://ansinet.com/itj

ITJ

ISSN 1812-5638

INFORMATION TECHNOLOGY JOURNAL

ANSInet
Asian Network for Scientific Information
308 Lasani Town, Sargodha Road, Faisalabad - Pakistan

Information Technology Journal 12 (4): 672-679, 2013
ISSN 1812-5638 / DOI: 10.3923/itj.2013.672.679

Fusion Method for Visible Light and Infrared Images Based on Compressive Sensing of Non-subsampled Contourlet Transformation Sparsity

[1]Xin Feng, [1]Xiaoming Wang, [2]Jianwu Dang and [2]Yu Shen
[1]Lanzhou University of Technology, China
[2]Lanzhou Jiaotong University, China

Abstract: A non-sub sampled Contour let coefficient compressive sensing based on infrared and visible image fusion method was proposed to solve the problem that the infrared light sensor and the visible light sensor was failed to get clear images simultaneously in this study. Firstly, the multiscale and multi-directional image decomposition for the infrared and visible image was preformed by using the non-sub sampled Contourlet transformation and then the non-subsampled Contourlet coefficients of them were obtained. Secondly, the Low-frequency coefficients of the infrared and visible images was fused by the weighted average fusion method and the band-pass sub-band coefficients was fused by the pseudo-random Fourier matrix observations weights fusion method; Thirdly, the coefficient reconstruction for the fused band-pass sub-band coefficients was carried out. Finally, the image was reconstructed by the inverse non-subsampled Contourlet transformation. The experiment results showed that this fusion algorithm was failed to get image with clear object and background and it had the low computational complexity and good fusion effect.

Key words: Signal processing, contourlet transformation, compressive sensing, fusion image

INTRODUCTION

Image fusion uses the different imaging modes of multi-sensor to provide complementary information and increase the amount of the image information for the further processing. It has been widely used in areas such as machine vision, geographic information system and biomedical engineering etc. The visible light and the infrared light have the different imaging mechanism, the former is imaged by the spectral reflectance and the latter is imaged by the thermal radiation. Therefore, the visible light images usually have abundant background information which can describe the environment in the scene better and the infrared image can clearly describe the existence of the target. The identification ability for the target and the interpretation ability for the environment are improved by the fusion of the visible light image and the infrared light image based on the complementary nature of the two kinds of images (Li *et al*., 2009).

Because of the limitation of the wavelet theory, several new multi-scale analysis methods have been proposed over the past decade such as rideglet transformation (Candes, 1998), curvelets transformation (Starck *et al*., 2002), Contourlet Transformation (CT) (Do and Vetterli, 2005), Non-subsampled Contourlet Transformation (NSCT) (Da Cunha *et al*., 2006), wave atoms transformation (Demanet and Ying, 2007), shearlets transformation (Easley *et al*., 2008) etc. Compared with the traditional wavelet transformation theory, these methods have the characteristics of multi-scale, time-frequency localization, multi-direction and anisotropy. By these methods, the image can effectively show its high singularity and fully express its structural information. At home and abroad, a considerable amount of researches have been done in the area of the multi-scale fusion (Li *et al*., 2009).

Zhang and Guo (2007) proposed a visible light image and infrared image fusion method that different rules were used on the separated NSCT coefficients. Fu and Zhao (2009) mentioned a novel image fusion algorithm based on the second generation curve let transform by the physical characteristics of infrared and visible imaging sensors. Firstly, the fast discrete curvelet transform was performed on the original images respectively to obtain the sub-band coefficients at different scales and in various directions. Then for low frequency sub-band coefficients, the fusion weights were determined by the target characteristics of infrared image and the detail information of visible image; while for high frequency sub-band coefficients, a fusion rule based on local region energy matching was employed. Jingchao and Shiru (2011) improved a visible light image and infrared image fusion method based on the Curvelet transformation and the adaptive PCNN. They

Corresponding Author: Xin Feng, Lanzhou University of Technology, LAN Zhou, 730050, China

fused the two types of image by conducting the weighted averages of their low-frequency sub-band coefficients. Then they selected their high frequency coefficients as the inputs to PCNN by using its global coupling characteristics and pulsed synchronization characteristics and also selected regional energy measurements as the connection strengths of PCNN. They got respectable results.

With the development of the information technology, the traditional image fusion methods have to process large amount of data than ever. So the requirement for the signal sampling, transmission and storage has been put into a higher level. A most vital and urgently solved problem is how to relieve this press, while effectively abstract the available information from the signals. The Compressive sensing theory proposed by Donoho (2006) and Candes and Wakin (2008) offered an effective way to solve this problem.

It is well known that the traditional digital signal processing frame is on the basis of the Nyquist sampling theorem. That is, in order to recover the original continuous signal from the discrete time signal sampled from the continuous signal, the sampling frequency must be greater than twice the signal bandwidth. And the Compressive sensing is a new way to convert the analogy signals into digital forms economically. It need not completely sample the signal and it needs not any priori information before the sampling. Therefore, the Compressive sensing greatly reduces the cost and complexity of the image acquisition system and decreases the image storage space and transmission cost (Donoho, 2006; Candes and Wakin, 2008). At present, the researchers have been done a great deal of studies on the compressed sensing in different areas. But very few research has been done on the area that applying the compressed sensing theory to the image fusion. Wan *et al*. (2008) firstly did image fusion by the compressed sensing but the author used the fusion rule by computing the weighted standard deviation of the image observation. The fusion effect was not so remarkable. And the convergence rate of the algorithm is slow.

This study proposed a novel method that using the non-subsampled contourlet (NSCT) based compressed sensing algorithm to do image fusion. The experiment results show that this algorithm can effectively improves the convergence rate, decreases the amount of processing data and raises the fusion effect.

The basic theory of the compressed sensing: The compressed sensing is a non-adaptive, nonlinear reconstruction sparse signal method, the main idea of the aforementioned method is that realizing the sample and compress by projecting the N dimensional signal to the measurement matrix and then obtaining the M dimensional observation vector. The process is shown in Fig. 1. The reconstruction process is the approximately accurate reconstruction of the original signals by using the optimization algorithm in the signal sparse decomposition instead of the simple linear calculation.

In order to simplify the problem, assume that the discrete real signal can be shown as the Eq. 1 and the sparsely K is under consideration:

$$x \epsilon R^{N\times 1},\ \|\Psi^T x\|_0 \leq K \leq N \quad (1)$$

where, N is the signal length, $\|.\|_0$ is the zero norm of the signal, that is the number of the signal value which is not equal to 0. Ψ is the sparse base of the signal, the m times measuring of which is:

$$y = \Phi x \quad (2)$$

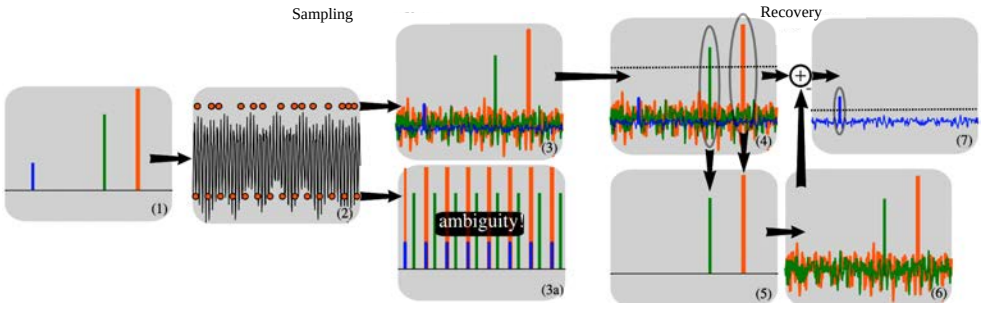

Fig. 1: The sample and recovery of the compressed sensing, 1-7: Show the steps of procedure

where, $\Phi \epsilon R^{m \times N}$ is the measurement matrix which is not relevant with Ψ and $m<N$. Assume that the observation vector y and the measurement matrix Φ are known and Φ satisfy the Restricted Isometry Property (RIP), the optimization algorithm with the zero norms can be used to reconstruct or approach the original signals:

$$\text{argmin} \|\Psi^t x\|_0, \quad \text{s.t.} \quad y = \Phi x \tag{3}$$

NSCT filters: The NSCT has all the characteristics of the traditional Contourlet transformation. It also has the feature of the translation invariance which can effectively reduce the influence the image registration error on the fusion performance (Zhang and Guo, 2008). In addition, the image decomposed by the NSCT has the same size with the original image which can easily get the correspondences among them. The fusion rule can be quickly determined by these correspondences. Therefore, NSCT is suitable for the image fusion.

Similar to the Contourlet transformation, the scale decomposition and the direction decomposition can be done separately in the NSCT. Firstly, the Non-subsampled Pyramid Filter Bank (NSPFB) was used to do multi-scale decomposition on the image. Then, the Non-subsampled Directional Filter Bank (NSDFB) was used to do direction decomposition on the multi-scale sub-band image and the subband coefficients in different direction and scale is obtained consequently.

The NSPFB mainly consists of the decomposition filter $\{H_0(z), H_1(z)\}$ and the synthesis filter $\{G_0(z), G_1(z)\}$ and the Bezout identical equation is satisfied. The decomposed construction of the NSPFB is shown in Fig. 2.

The NSPFB filter with k level decompositions is used to get k+1 sub-band images with the same size as the original image:

$$H_0(z)\, G_0(z)+H_1(z)\, G_1(z) = 1 \tag{4}$$

For the sub-band image in certain scale, the NSPFB filter with the l level decompositions is used to get 2^l sub-band images with the same size as the original image:

$$U_0(z)\, V_0(z)+U_1(z)\, V_1(z) = 1 \tag{5}$$

The decomposed construction of the NSPFB is shown in Fig. 3.

The multi-scale decomposition and the multidirectional decomposition on the signals can be preformed by the combined use of the NSPFB and the NSDFB.

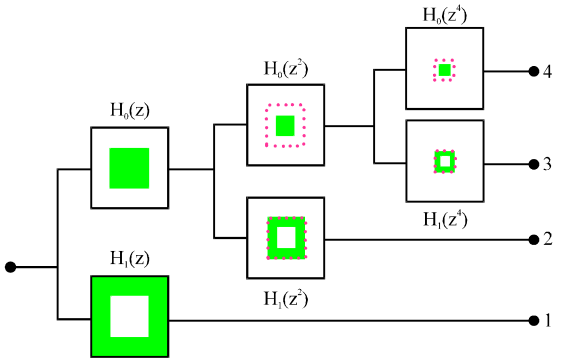

Fig. 2: The analysis part of NFPFB

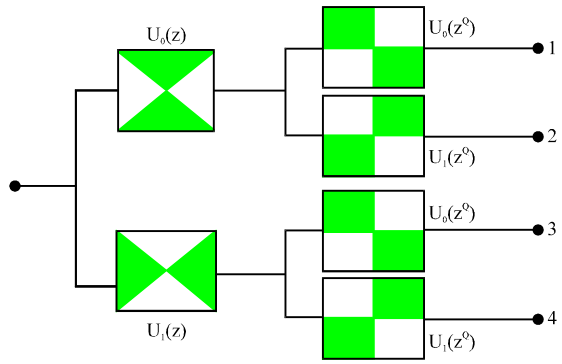

Fig. 3: The analysis part of NSDFB

The fusion method based on compressed sensing: The low and high frequency coefficients can be obtained by the NSFB decomposition. The high frequency coefficients are the sparse signals, while the low frequency coefficients are the approximation signals with low sparsely. If they multiply together with the observation matrix, the correlation among the coefficients of the low frequency components would be broken and the reconstruction effect would be degraded. Thus, the low and high frequency sub-band is processed separately to get the better construction effect.

SELECTION METHOD FOR THE LOW FREQUENCY SUB-BAND COEFFICIENT

The low frequency sub-band coefficients which contain the main energy of the image can be fused directly for its low sparsely. By the simple average method, the fusion image contrast ratio would be degraded. Furthermore, the effect would be much worse because of the opposite polarity in certain area in the infrared ray and visible light region. In this study, the weighted average coefficients based on the infrared ray and visible light

physical properties is used to fuse the low frequency sub-band coefficient, the fused coefficients $C_{j_0}^{I\_F}(k_1,k_2)$ are shown as follows:

$$C_{j_0}^{I\_F}(k_1,k_2)=\frac{C_{j_0}^{I\_v}(k_1,k_2)w_{I\_v}(k_1,k_2)+C_{j_0}^{IR}(k_1,k_2)w_{IR}(k_1,k_2)}{w_{I\_v}(k_1,k_2)+w_{IR}(k_1,k_2)} \quad (6)$$

where, $w_{I\_v}(k_1, k_2)$, $w_{IR}(k_1, k_2)$ are defined as follows:

$$w_{I\_v}(k_1,k_2)=\frac{\left|C_{j_0}^{I\_v}(k_1,k_2)\right|\left(1+\sigma_{I\_v}(k_1,k_2)\right)}{\max\left(\left|C_{j_0}^{I\_v}(k_1,k_2)\right|/\left(1+\sigma_{I\_v}(k_1,k_2)\right)\right)} \quad (7)$$

$$w_{IR}(k_1,k_2)=\frac{\left|C_{j_0}^{IR}(k_1,k_2)-\overline{C}_{j_0}^{IR}(k_1,k_2)\right|\left(1+\sigma_{IR}(k_1,k_2)\right)}{\max\left(\left|C_{j_0}^{IR}(k_1,k_2)-\overline{C}_{j_0}^{IR}(k_1,k_2)\right|/\left(1+\sigma_{IR}(k_1,k_2)\right)\right)} \quad (8)$$

where, $\overline{C}_{J0}(k_1, k_2)$ and $\sigma(k_1, k_2)$ denote the mean and standard deviation of the coefficients in NSFT field.

SELECTION METHODS FOR THE BAND-PASS DIRECTION SUB-BAND COEFFICIENTS

The observation of the high frequency sub-band coefficients: The high frequency sub-band coefficients can be considered as sparse and can be observed by the Compressed Sensing. The decomposed low frequency coefficients have weak sparseness, that is, there is significant correlation among these coefficients. In order to better construct the image contour and hold the image energy information, the tower filter take one layer decomposition and the direction decomposition of 3 levels. Then the direction sub-band number of the high frequency sub-band is $2^3 = 8$. The high frequency sub-band coefficients $C^{\omega}_{H\_v}$ and $C^{\omega}_{H\_R}(\omega = 1, 2, 3,..., 8)$ of the infrared ray and visible light with the size of are lined as 8 column vectors, respectively, the size of each column vectors is $(N^2/9)\times 1$. Then these 8 sub-band coefficients in high frequency direction are calculated by Pseudo-random Fourier matrix. The sub-band coefficients column vector observations Z_I^{ω} are obtained, the sizes of which are. They are denoted as follows:

$$Z_I^{\omega} = \Phi\, C_I^{\omega} \quad (9)$$

For the NSCT, the larger of the decomposed high frequency sub-band coefficient value, the more of the information contained in the image. Because the observation process for the compressed sensing the image signal is linear, thus the relationship among observations can be considered as a linear relationship. So the larger of the observation value, the more of the information contained in the image. The obvious image characteristics such as straight line, curve, contour, area etc are usually denoted as the variation of gradation in the original image. However, the image characteristics are denoted as the high frequency sub-band transformation coefficients with large scale in the multi-scale transform domain. Although, the observations transformed from the high frequency coefficients still remain their linear relationship, there is no correlation between the observation matrix and the NSCT transform domain. Thus, the fusion rules could not be chosen by the relationship among the pixels and the NSCT coefficients. In this study, the weighted fusion method is adopted according to the linear relationship among the observations.

Firstly, the weighted fusion of the visible light image is supposed as follows:

$$w_v^{\omega} = \frac{\left|z_v^{\omega}\right|}{\left|z_v^{\omega}\right| + \left|z_R^{\omega}\right|} \quad (10)$$

The weighted fusion of the infrared images is:

$$w^{\omega}_R = 1 - w_v^{\omega} \quad (11)$$

The high frequency sub-band coefficients observations was observed after the weighted fusion on sub-band coefficients in 8 high frequency directions of the visual light images and infrared images. The results are shown as follows:

$$z^{\omega} = w_v^{\omega} z_v^{\omega} + w^{\omega}_R z^{\omega}_R \quad (12)$$

where, z_v^{ω}, z^{ω}_R are the coefficient observations in 8 high frequency directions of the visual light images and the infrared images respectively. While, w_v^{ω}, w^{ω}_R are the weighted fusion values in the corresponding directions. z^{ω} is the fused high frequency sub-band observations.

The reconstruction of the high frequency sub-band coefficients: The key of the high frequency sub-band observations construction algorithm is solving optimization problems:

$$\min_{x\in R^n} \sum|\Psi x|, \text{st.}\Phi x = y \quad (13)$$

where, Ψ is sparse transform matrix (the NSDFB filter matrix in NSCT transformation is selected in this study), x is the sparse form of the signals, Φ is the observation matrix, y is the observation value. This is a real isotropic Total Variation (TV) model.

According to the study (Nocedal and Wright, 2006), the algorithm in this study used the method of Lagrange

Multipliers to solve the augmented Lagrange function. The basic algorithm is shown as follows:

While "do not converge" Do
- Approach the minimum of the augmented Lagrangian function by the Alternating Direction method.
- Update the multipliers

End Do

Replacing $\|.\|_2$ by $\|.\|$ to simplify the calculation, then the TV model is equivalent to the Eq. 14:

$$\min_{\omega_i \in R^2, x \in R^n} \sum_i \|\omega_i\|, \text{s.t.} \Phi x = y \ \& \ \Psi x = \omega_i \quad (14)$$

The corresponding augmented Lagrange problem is:

$$\min_{\omega_i, x} \sum_i \left(\|\omega_i\| - v_i^T (\Psi x - \omega_i) + \frac{\beta}{2} \|\Psi x - \omega_i\|^2 \right) - \lambda^T (\Phi x - y) + \frac{\mu}{2} \|\Phi x - y\|^2 \quad (15)$$

The alternating minimization method is used to solve Eq. 13. For a fixed x, the optimal value ω_i in all i is obtained by solving the Eq. 16:

$$\omega_i = \max \left\{ \left\| \psi_i x - \frac{v_i}{\beta} \right\| - \frac{1}{\beta}, 0 \right\} \frac{\psi_i x - v_i / \beta}{\|\psi_i x - v_i / \beta\|} \quad (16)$$

Suppose $\hat{u}$ and $\{\hat{u}_i\}$ are the approximate solutions of Eq. 13, the multipliers of which are updated by the Eq. 17. All of i satisfy the Eq. 17:

$$v_i \leftarrow v_i - \beta(\Psi_i \hat{x} - \hat{\omega}_i), \ \lambda \leftarrow \lambda - \mu(A \hat{x} - y) \quad (17)$$

Furthermore, the reconstructed high frequency direction sub-band coefficients can be obtained by combining the algorithm in study (Nocedal and Wright, 2006).

RECONSTRUCTION OF NSFT

The NSFB high frequency direction sub-band coefficients $C^{\omega}_F(\omega = 1,2,3,..., 8)$ are obtained by the reconstruction of the fused observations. The low frequency sub-band coefficients of the fused visual light images and infrared images and the sub-band coefficients in 8 high frequency directions are in the column vector forms. Translating them into the matrix forms of (N/3)×(N/3) and then combining them into a coefficient matrix with the size of N×N. The resulting images of the fused visual light images and infrared images are obtained by the reconstruction of the inverse NSCT transformation.

EXPERIMENT RESULTS AND ANALYSIS

In this algorithm, the Pseudo random Fourier matrix is used to do compressed sensing sampling, As shown in Fig. 4. The pseudo random down-sampling is the polynomial variable density random sampling. It subject to the probability density function that doing intensive sampling in low frequency signal and sparse sampling in high frequency signal. This can greatly reduce the computational complexity.

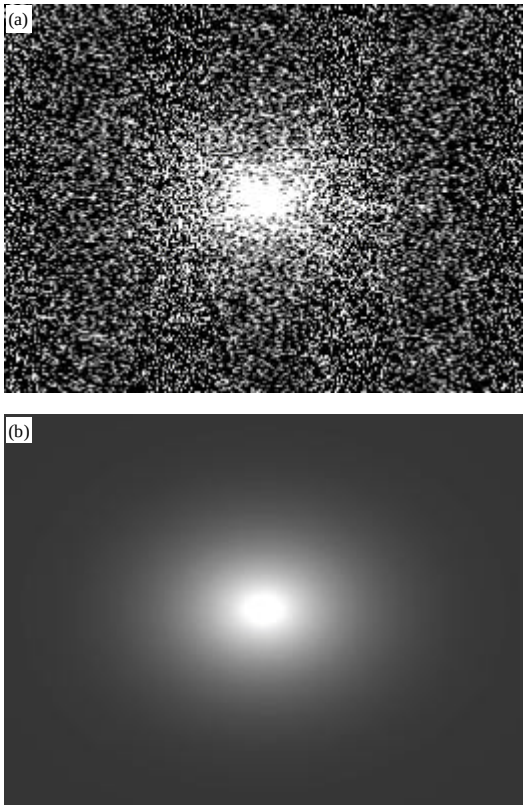

Fig. 4(a-b): Observation matrix (a) Fourier sampling model and (b) 2D probability density function

In order to verify the effectiveness and correctness of the algorithm, two groups of visual light images and infrared images are chosen to do the fusion experiment. The images adopted in the experiment were the Equinox faces and the Octec. The computer in the experiment used the Windows XP operating system, Pentium(R) Dual-Core E5400@ 2.70 GHz, 2.69 GHz CPU, 2 G memory. The programming platform was the MATLAB7.0.1. In the fusion experiment, this algorithm is compared with the LP (Laplacian Pyramid) method, the NSCT method and the CS-SD method. Where, the LP method used 3 layers decomposition, the high frequency took the maximum value and the low frequency took the average value. The NSFT method adopted the Parameter set standard mentioned in study (Zhang and Guo, 2008), by the 3 layer image decomposition. The decomposition levels used from the coarsest scale to the finest scale are 2, 3 and 3.

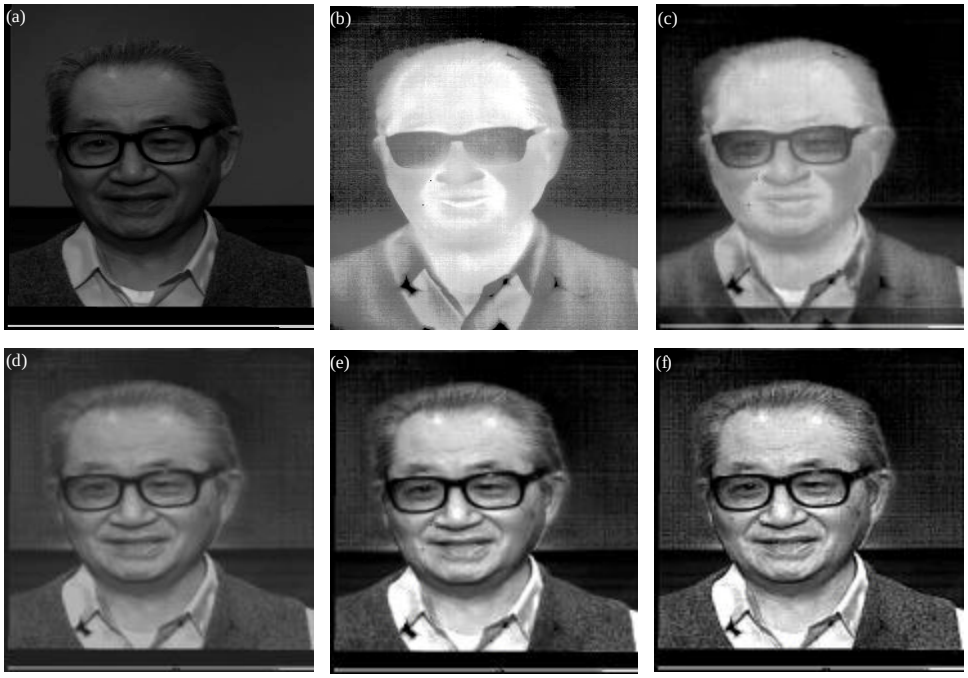

Fig. 5(a-f): The contrast of several methods (a) Visible image, (b) Infrared image, (c) Method of LP, (d) Method of NSCT, (e) Method of CS-SD and (f) Present approach

The "maxflat" filter was adopted as the scale decomposition filter and the "dmaxflat" filter was adopted as the direction decomposition filter. The sampling rate was chosen as 0.3 in the CS-SD method according to study (Li, 2011). In this algorithm, the sampling rate was 0.15. The data used in the image recovery are 30% of the total image data. The filter used in our algorithm was same as the study (Zhang and Guo, 2008).

Figure 5 shows the fused images of the Equinox faces. Figure 5a is the visible light image. Figure 5b is the infrared image. Figure 5c is the fused result by the LP method. In Fig. 5, there are ghosting, block fuzzy and obvious detail loss. Figure 5d is the fused result by the NSCT method. Compared with the CP method, the ghosting and block fuzzy has been eliminated and the clarity has been advanced. It shows the edge capture capability. Figure 5e is the fused result by the CS-CD method; its visual effect is obviously higher than the former two images. Figure 5f is the fused result by the algorithm in this study. Compared with the former three images, it has the highest contrast and the complete contour. This method even obtained subtle details of the image.

Figure 6 is the fusion results of the Octec. Figure 6a is the visible image. Figure 6b is the infrared image. The results of these methods are shown in Fig. 6. In Fig. 6c, the result of the LP method is relatively blurred with much distortion and low contrast. In Fig. 6d, the result of the NSCT has better effect than PL method in certain spatial details such as the preserving of the edge and the removing of the virtual shadow. In the decomposition and the reconstruction process, the down-sampling and up-sampling is taken off in the NSCT method to avoid the frequency aliasing effect. In Fig. 6e, the result of the CS-SD has the higher contrast and clearer details. In Fig. 6f, the algorithm in this study has smooth edges and completely removes the virtual shadow.

Figure 7 shows the effects of the local area enlarged images fused by all of the methods. Figure 7a is the fusion result of PL method. It has obvious ghost and blur. Figure 7b is the fusion result of NSCT method in study (Zhang and Guo, 2008). It has clear contour, better preserved edges and hardly any ghost. Figure 7c is the result of CS-SD fusion method in study (Li, 2011). It has more smooth edges, less distortion and higher contrast. Figure 7d is the result of the method in this study. It is obvious that the image better preserved the edges and eliminated the edge shock. It has the best visual effects of all the 5 methods. In order to better analysis the fusion performance, the 5 algorithms is evaluated by the methods in study (Zhang and Guo, 2008) with the index of Information Entropy (IE), Average

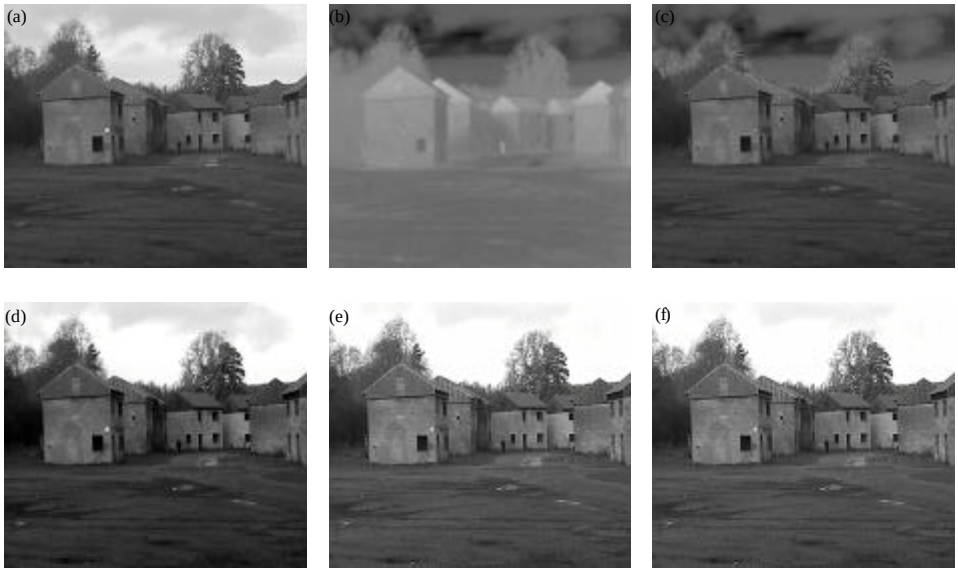

Fig. 6(a-f): The contrast of several methods (a) Visible image, (b) Infrared image, (c) Method of LP, (d) Method of NSCT, (e) Method of CS-SD and (f) Present approach

Fig. 7(a-d): The fusion contrast of local region (a) Method of LP, (b) Method of NSCT, (c) Method of CS-SD and (d) Present approach

Gradient (AG), Mutual Information (MI), Edge retention (Q) and computation time (T).The results are shown as Table 1.

For all of the indexes, the algorithm in this study has the highest levels except the MI. The MI of this algorithm is a little lower than that of the NSCT method. It is shown that the fusion method in this study has better information acquisition performance and detail expression performance. In the index of computation time, this algorithm costs far lower time than the NSCT and

Table 1: Evaluation criterion of fusion results

Methods	Information entropy	Average gradient	Mutual information	Q(Edge retention)	T/s(computationtime)
Laplacian pyramid	5.88	0.007	1.86	0.31	1
Non-subsampled contourlet transformation	6.54	0.013	2.48	0.39	126
CS-CD (Compressed sensing)	6.76	0.017	2.43	0.41	59
This study	6.82	0.018	2.36	0.44	16

CS-MAV fusion method. In a word, the algorithm in this study has low computational complexity and good fusion effect.

CONCLUSION

The compressed sensing theory is applied to the image fusion in this study. Compared with the tradition fusion method, the hypothesis of the priori information is not necessary in this algorithm. Furthermore, the image data are reduced after the observation and the computational complexity is reduced effectively. In the choice of the transform domain, the NSCT used in this algorithm has the translational invariance which can lower the matching and fusion error influence on the fusion performance and easily get the corresponding relationship among sub-bands which benefits to the set of the fusion rules. The experiment results show that the NSCT transform domain based Compressed Sensing has good effect on image fusion. In deed, the applications of the Compressed Sensing in image fusion are still at the exploration stage. It has huge potentiality in the image fusion with the development of the Compressed Sensing theory.

REFERENCES

Candes, E.J. and M.B. Wakin, 2008. An introduction to compressive sampling. IEEE Signal Process. Mag., 25: 21-30.

Candes, E.J., 1998. Ridgelets: Theory and applications. Technical Report No. 1998-17, Stanford University, California.

Da Cunha, A.L., J.P. Zhou and M.N. Do, 2006. The non subsampled contourlet transform: Theory, design and applications. IEEE Trans. Image Process., 15: 3089-3101.

Demanet, L. and L.X. Ying, 2007. Wave atoms and sparsely of oscillatory patterns. Appl. Comp. Harm. Anal., 23: 368-387.

Do, M.N. and M. Vetterli, 2005. The contourlet transform: An efficient directional multiresolution image representation. IEEE Trans. Image Process., 14: 2091-2106.

Donoho, D.L., 2006. Compressed sensing. IEEE Trans. Inform. Theory, 52: 1289-1306.

Easley, G., D. Labate and W.Q. Lim, 2008. Sparse directional image representations using the discrete shearlet transform. Appl. Comp. Harm. Anal., 25: 25-46.

Fu, M.Y. and C. Zhao, 2009. Fusions of infrared and visible images based on the second generation Curvelet transform. J. Infrared Millimeter Waves, 28: 254-258.

Jingchao, Z. and Q. Shiru, 2011. A better algorithm for fusion of infrared and visible image based on curvelet transform and adaptive pulse coupled neural networks. J. Northwestern Polytech., Univ., 29: 123-128.

Li, H.H., L. Guo and K. Liu, 2009. SAR and optical image fusion based on curvelet transform. J. Optoelectron. Laser, 20: 1110-1113.

Li, X., 2011. Efficient fusion for infrared and visible images based on compressive sensing principle. IET Image Process., 5: 141-147.

Nocedal, J. and S.J. Wright, 2006. Numerical Optimization. Springer-Verlag, New York, USA., pp: 188-193.

Starck, J.L., E.J. Candes and D.L. Donoho, 2002. The curvelet transform for image denoising. IEEE Trans. Image Process., 11: 670-684.

Wan, T., N. Canagarajah and A. Achim, 2008. Compressive images fusion. Proceedings of the 15th IEEE International Conference on Image Processing, October 12-15, 2008, San Diego, CA, USA., pp: 1308-1311.

Zhang, Q. and B. Guo, 2008. A remote sensing image fusion algorithm based on the non-subsampled Contourlet. J. Optics, 28: 74-80.

Zhang, Q. and B.L. Guo, 2007. Fusion of infrared and visible light images based on nonsubsampled Contourlet transform. J. Infrared Millimeter Waves, 26: 476-480.